Supporting Information

A Series of Bimetallic Ammonium RbEu Nitrates Exhibiting Switchable Dielectric Constant and Photoluminescence Properties†

Hua-Kai Li, Li-Ping Wang, Zong-Ze Cui, Qi Xu, Liang-Liang Zou, Na Wang, Le-Ping Miao, Heng-Yun Ye,* and Chao Shi*

Chaotic Matter Science Research Center, International Institute for Innovation, Jiangxi University of Science and Technology, Nanchang 330000, Jiangxi Province, P.R. China.
*Foundation Item: National Natural Science Foundation of China (No. 22175079 and 22275075) and Natural Science Foundation of Jiangxi Province (No. 20225BCJ23006, 20224ACB204002 and 20204BCJ22015).
E-mail address: 15150517670@163.com
Tel.: 0791-83858326

More characterizations

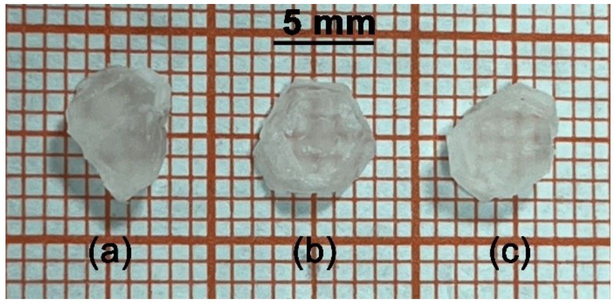

Fig S1. The macroscopic shape of the single crystal of crystal (a) **1**, (b) **2** and (c) **3**.

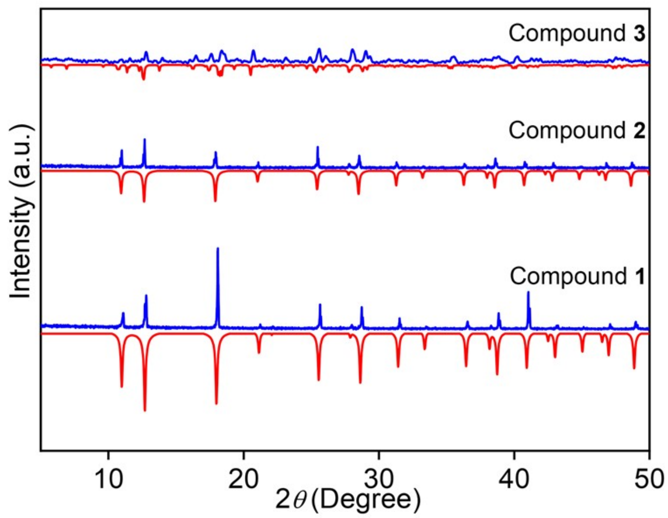

Fig S2. The powder X-ray diffraction (PXRD) patterns for **1−3** measured at room temperature. Notes: blue lines (Measurement); red lines (Simulation).

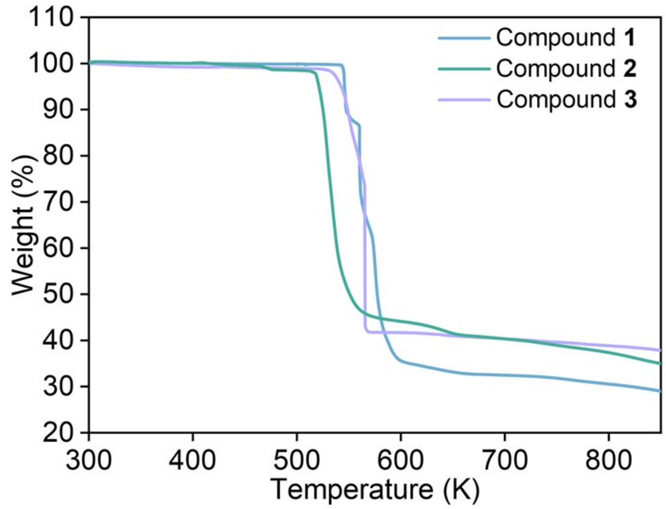

Fig S3. The thermogravimetric (TG) curves of **1**−**3**.

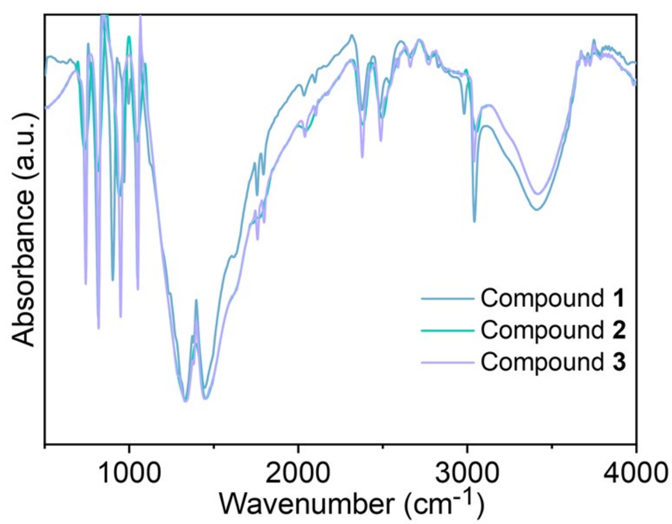

Fig S4. FTIR spectra of **1**−**3**.

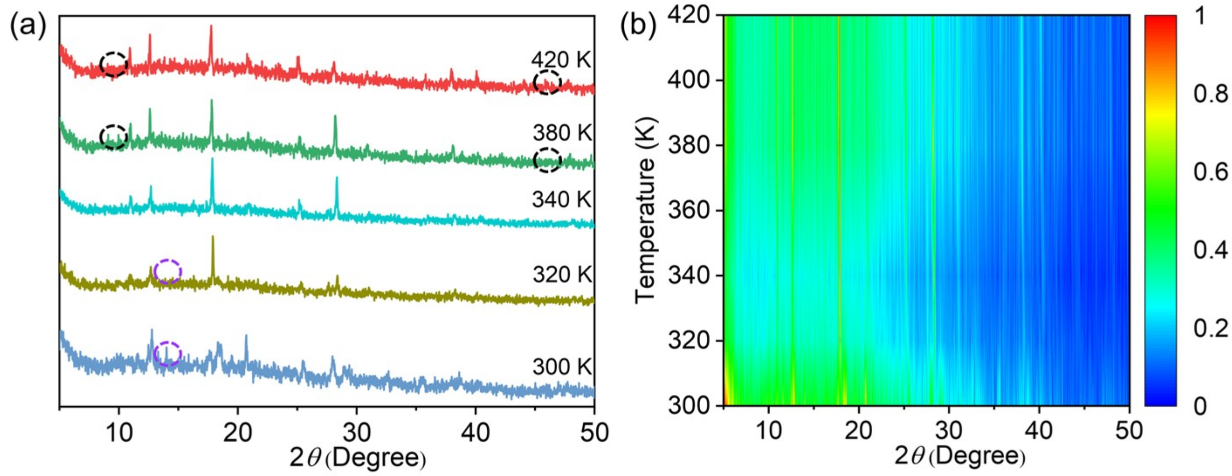

Fig. S5. (a) Variable-temperature PXRD spectra of **3** collected on cooling mode. (b) False-color maps extracted at 5–50° intervals of the temperature-variable PXRD pattern.

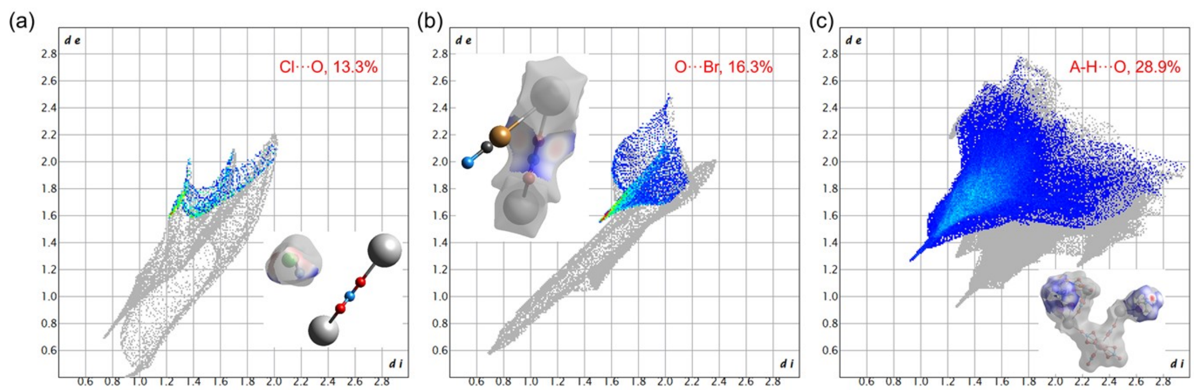

Fig S6. Hirshfeld surface analysis of (a) Cl, (b) Br and (c) I atoms substitutions, interaction forces between organic cations and nitric radicals. Red, white and blue regions of the Hirshfeld surfaces correspond to positive (close contact), neutral and negative isoenergies, respectively. In the fingerprint plots, di and de denote the distances to the nearest atom inside and outside of the Hirshfeld surface, respectively.

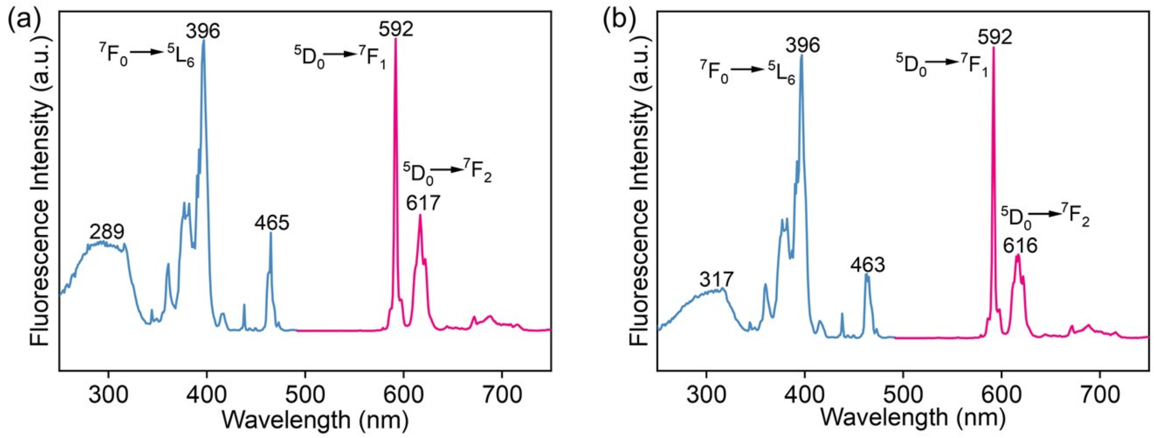

Fig S7. The photoluminescence properties of **2** and **3** at room temperature. Emission (λ_{exc} = 396 nm) and excitation (λ_{em} = 592 nm) spectra of (a) **2** and (b) **3**. Notes: the red and blue lines represent emission and excitation spectra, respectively.

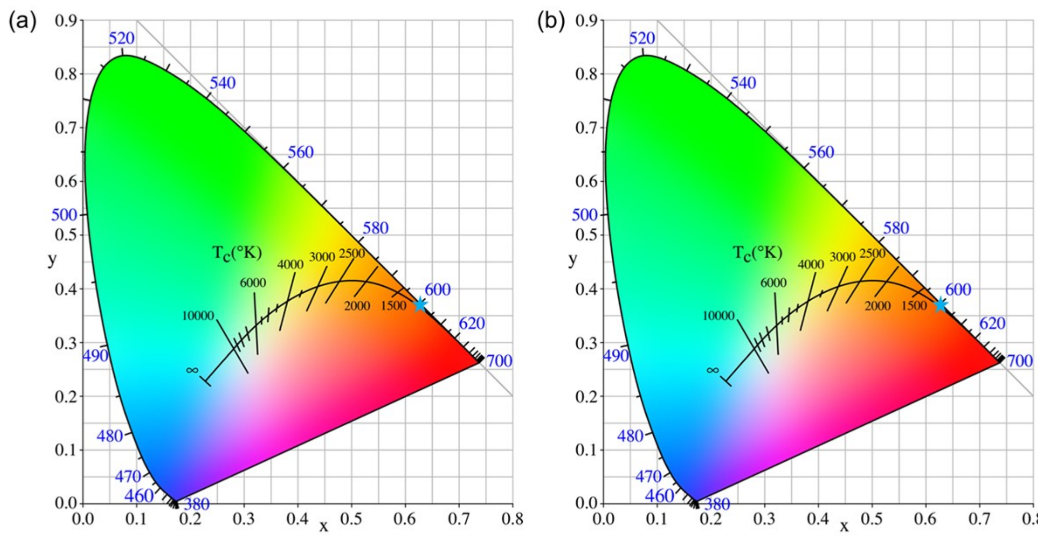

Fig S8. CIE chromaticity diagram of (a) **2** and (b) **3** polycrystalline phosphors excited by UV light.

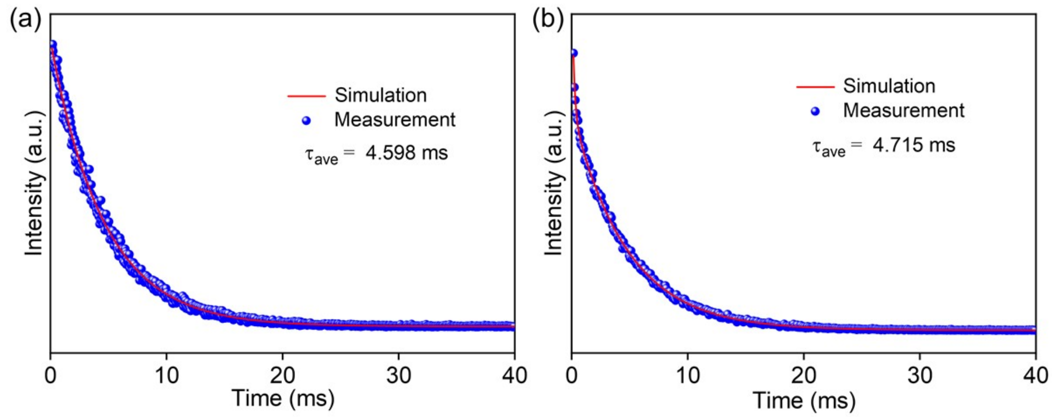

Fig S9. Photoluminescence decay lifetime curves of (a) **2** and (b) **3**.

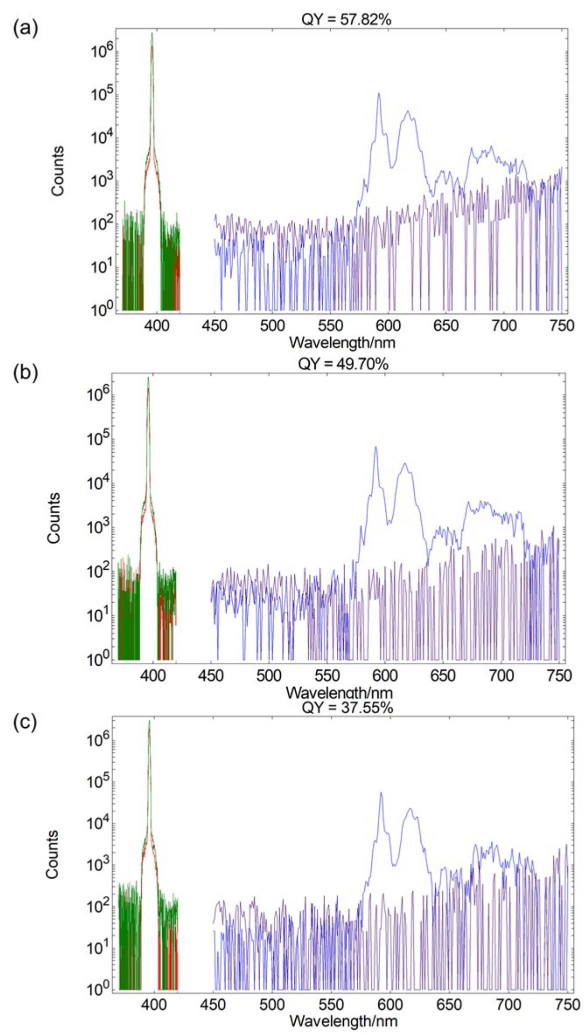

Fig S10. The FQY of (a) **1**, (b) **2** and (c) **3**.

Table S1. The averaged enthalpy changes and corresponding entropy changes in **1**−**3**. Using the Boltzmann equation, $\Delta S = R \cdot \ln N$, the N value of **1**−**3** is estimated.

Compound	**1**	**2**	**3**
ΔH (kJ·mol^{-1})	8.7989	12.0577	9.1380
ΔS (J·mol^{-1}·K^{-1})	34.8472	43.6084	28.1517
N	66.1145	189.6493	29.5493

Table S2. Comparison of structural phase transition temperatures of rare-earth double perovskite materials.

Formula[a]	T/K	Ref
$(DMP)_2LaRb(NO_3)_6$	219/209	1
$(HQ)_2RbEu(NO_3)_6$	254/245	2
$[(CH_3)_3NCH_2Cl]_2RbEu(NO_3)_6$	259/246	This work (**1**)
$(HQ)_4KEu(NO_3)_8$	263/259, 292/290	3
$(RM3HQ)_2RbPr(NO_3)_6$	280/279	4
$(RM3HQ)_2RbLa(NO_3)_6$	280/269, 425/409	5
$[(CH_3)_3NCH_2Br]_2RbEu(NO_3)_6$	281/272	This work (**2**)
$(RM3HQ)_2RbCe(NO_3)_6$	285/272	6
$(RM3HQ)_2RbEu(NO_3)_6$	285/279	7
$(R3HQ)_4KCe(NO_3)_8$	323/306	8
$[(CH_3)_3NCH_2I]_2RbEu(NO_3)_6$	327/310, 405/377	This work (**3**)
$(RM3HQ)_2KEu(NO_3)_6$	371/363	9
$(R3HQ)_4CsEu(NO_3)_8$	375/359	10
$(R3HQ)_4CsSm(NO_3)_8$	379/358	10
$(4FHQ)_2RbEu(NO_3)_6$	432/418	2
$(3HQ)_4RbEu(NO_3)_8$	442/434	11

[a] DMP = *N*,*N*-dimethylpyrrolidinium cation; HQ = quinuclidium; RM3HQ = (*R*)-*N*-methyl-3-hydroxylquinuclidinium; R3HQ = (*R*)-3-hydroxylquinuclidinium cation; 4FHQ = 4-fluoro-quinuclidium.

Table S3. Crystal data and structure refinement details of **1**, **2** and **3**.

1	193 K	293 K
Formula	$C_8H_{22}Cl_2EuN_8O_{18}Rb$	$C_{16}Cl_4Eu_2N_{16}O_{36}Rb_2$
Formula weight	826.68	1608.94
T / K	192.97(10)	293(2)

Crystal system	monoclinic	cubic
Space group	*I*2/*m*	*Fm*-3*m*
a / Å	9.9367(13)	13.9355(2)
b / Å	9.6137(13)	13.9355(2)
c / Å	13.8856(15)	13.9355(2)
α / °	90	90
β /°	95.863(10)	90
γ /°	90	90
V / Å^3	1319.5(3)	2706.25(12)
Z	2	2
D_{calc} / g·cm^{-3}	2.081	1.975
μ / mm^{-1}	4.502	4.388
F(000)	808.0	1528.0
θ range / °	4.816−49.98	5.062−62.68
Reflns collected	4111	2583
Independent reflns (R_{int})	1226 (0.0538)	256 (0.0124)
no. parameters	131	26
R_1[a], wR_2[b] [I>2σ(I)]	0.2346, 0.5006	0.0375, 0.1011
R_1, wR_2 [all data]	0.2428, 0.5148	0.0375, 0.1011
GOF	2.542	1.175
$\Delta\rho$[c] / e·Å^{-3}	24.41, −3.56	1.09, −1.03
CCDC	2310567	2310568

2	293 K
Formula	$Br_4C_{16}Eu_2N_{16}O_{36}Rb_2$
Formula weight	1786.80
T / K	293(2)
Crystal system	cubic
Space group	*Fm*-3*m*
a / Å	13.9993(6)
b / Å	13.9993(6)
c / Å	13.9993(6)
α / °	90
β /°	90
γ /°	90
V / Å^3	2743.6(4)
Z	2
D_{calc} / g·cm^{-3}	2.163
μ / mm^{-1}	7.047
F(000)	1672.0
θ range / °	5.04−62.694

Reflns collected	2703
Independent reflns (R_{int})	256 (0.0187)
no. parameters	23
R_1[a], wR_2[b] [I>2σ(I)]	0.0434, 0.1303
R_1, wR_2 [all data]	0.0438, 0.1305
GOF	1.169
$\Delta\rho$[c] / e·Å^{-3}	0.90, −0.95
CCDC	2310569

3	311 K
Formula	$C_8H_{22}EuI_2N_8O_{18}Rb$
Formula weight	1009.56
T / K	311.15
Crystal system	triclinic
Space group	P-1
a / Å	9.6573(3)
b / Å	14.1326(4)
c / Å	17.3712(5)
α / °	112.633(3)
β /°	104.666(3)
γ /°	93.116(2)
V / Å^3	2086.18(12)
Z	3
D_{calc} / g·cm^{-3}	2.411
μ / mm^{-1}	6.300
F(000)	1428.0
θ range / °	4.424−49.99
Reflns collected	17253
Independent reflns (R_{int})	7086 (0.0275)
no. parameters	526
R_1[a], wR_2[b] [I>2σ(I)]	0.0497, 0.1402
R_1, wR_2 [all data]	0.0578, 0.1470
GOF	1.019
$\Delta\rho$[c] / e·Å^{-3}	3.99, −2.41
CCDC	2314668

[a] $R_1 = \Sigma||F_o| - |F_c||/\Sigma|F_o|$. [b] $wR_2 = [\Sigma w(F_o^2 - F_c^2)^2/\Sigma w(F_o^2)^2]^{1/2}$. [c] Maximum and minimum residual electron density.

Table S4. Selected bond lengths [Å] and angles [°] for **1**, **2** and **3**.

1−193 K

Eu1−O6	2.45 (5)	Rb1−O3	2.66 (6)
Eu1−O1	2.43 (5)	Rb1−O4	2.67 (4)
Eu1−O2	2.43 (5)	$O6^{i}$−Eu1−$O6^{iii}$	34 (3)
$O6^{iii}$−Eu1−$O6^{ii}$	180.00 (19)	$O3^{viii}$−Rb1−$O4^{x}$	97.1 (11)
$O6^{i}$−Eu1−$O6^{ii}$	146 (3)	$O3^{ix}$−Rb1−$O4^{viii}$	97.1 (11)
$O6^{i}$−Eu1−$O6^{iv}$	179.99 (14)	O3−Rb1−O4	82.9 (11)
$O6^{ii}$−Eu1−$O6^{iv}$	34 (3)	$O3^{x}$−Rb1−O4	97.1 (11)
$O6^{iii}$−Eu1−$O6^{iv}$	146 (3)	$O3^{ix}$−Rb1−O4	97.1 (11)
$O1^{vii}$−Eu1−$O6^{iii}$	139.2 (16)	$O4^{x}$−Rb1−O4	180.00 (13)
O1−Eu1−$O6^{iv}$	139.2 (16)	$O4^{x}$−Rb1−$O4^{viii}$	180.00 (13)
$O1^{v}$−Eu1−$O6^{iii}$	40.8 (16)	$O1^{v}$−Eu1−$O6^{iv}$	110 (2)
O1−Eu1−$O6^{i}$	40.8 (16)	O1−Eu1−$O6^{ii}$	110 (2)
O1−Eu1−$O6^{iii}$	70 (2)	$O1^{vi}$−Eu1−$O6^{iii}$	110 (2)
$O1^{vi}$−Eu1−$O6^{i}$	139.2 (16)	O1−Eu1−$O1^{vii}$	91 (3)
$O1^{vi}$−Eu1−$O6^{iv}$	40.8 (16)	$O1^{vi}$−Eu1−$O1^{v}$	91 (3)
$O1^{v}$−Eu1−$O6^{i}$	70 (2)	O1−Eu1−$O1^{v}$	89 (3)
$O1^{vii}$−Eu1−$O6^{iv}$	70 (2)	$O1^{vi}$−Eu1−$O1^{vii}$	89 (3)
$O1^{vii}$−Eu1−$O6^{ii}$	40.8 (16)	$O1^{v}$−Eu1−$O1^{vii}$	180 (2)
$O1^{vii}$−Eu1−$O6^{i}$	110 (2)	O1−Eu1−$O1^{vi}$	180.0 (18)
$O1^{vi}$−Eu1−$O6^{ii}$	70 (2)	$O2^{vii}$−Eu1−$O6^{i}$	71 (2)
$O1^{v}$−Eu1−$O6^{ii}$	139.2 (16)	$O2^{vii}$−Eu1−$O6^{ii}$	87.8 (16)
$O2^{vi}$−Eu1−$O6^{i}$	92.2 (16)	O2−Eu1−$O6^{iii}$	109 (2)
$O2^{v}$−Eu1−$O6^{iii}$	87.8 (16)	$O2^{v}$−Eu1−$O2^{vi}$	103 (3)
$O2^{v}$−Eu1−$O6^{i}$	109 (2)	O2−Eu1−$O2^{v}$	77 (3)
O2−Eu1−$O1^{vi}$	132.2 (18)	O3−Rb1−$O3^{viii}$	90 (2)
O2−Eu1−O1	47.8 (18)	$O3^{x}$−Rb1−$O3^{viii}$	90 (2)

$O3^{viii}$–Rb1–O4	82.9 (11)	O3–Rb1–$O4^{viii}$	82.9 (11)

Symmetry codes: (i) *x*−1/2, *y*−1/2, *z*−1/2; (ii) −*x*+3/2, *y*−1/2, −*z*+5/2; (iii) *x*−1/2, −*y*+5/2, *z*−1/2; (iv) −*x*+3/2, −*y*+5/2, −*z*+5/2; (v) *x*, −*y*+2, *z*; (vi) −*x*+1, −*y*+2, −*z*+2; (vii) −*x*+1, *y*, −*z*+2; (viii) *x*, −*y*+3, *z*; (ix) −*x*+2, *y*, −*z*+2; (x) −*x*+2, −*y*+3, −*z*+2; (xi) *x*+1/2, *y*+1/2, *z*+1/2.

1–293 K

Rb1–O1	2.760 (18)	Eu1–O2	2.531 (8)
O1–Rb1–$O1^{iii}$	90.0	$O2^{xvi}$–Eu1–$O2^{xix}$	67.79 (17)
$O1^{iv}$–Rb1–$O1^{i}$	90.000 (3)	$O2^{xiv}$–Eu1–$O2^{xxi}$	80.05 (18)
$O1^{iv}$–Rb1–$O1^{v}$	90.0	$O2^{xxii}$–Eu1–$O2^{xix}$	40.9 (5)
O1–Rb1–$O1^{iv}$	180.0	$O2^{xvi}$–Eu1–$O2^{xxi}$	99.95 (18)
O1–Rb1–$O1^{v}$	90.000 (1)	O2–Eu1–$O2^{xv}$	145.8 (3)
$O1^{iii}$–Rb1–$O1^{iv}$	90.000 (1)	$O2^{xviii}$–Eu1–$O2^{xxi}$	67.79 (17)
$O1^{iii}$–Rb1–$O1^{i}$	90.000 (3)	$O2^{xx}$–Eu1–$O2^{xv}$	99.95 (18)
O1–Rb1–$O1^{ii}$	90.000 (3)	$O2^{xx}$–Eu1–$O2^{xxi}$	112.21 (17)
$O1^{ii}$–Rb1–$O1^{i}$	180.0	$O2^{xvii}$–Eu1–$O2^{xv}$	112.21 (17)
$O1^{iii}$–Rb1–$O1^{ii}$	90.000 (1)	O2–Eu1–$O2^{xxii}$	67.79 (17)
$O1^{iii}$–Rb1–$O1^{v}$	180.0	$O2^{xxii}$–Eu1–$O2^{xvii}$	34.2 (3)
$O1^{iv}$–Rb1–$O1^{ii}$	90.0	$O2^{xiv}$–Eu1–$O2^{xxii}$	99.95 (18)
$O1^{ii}$–Rb1–$O1^{v}$	90.000 (2)	O2–Eu1–$O2^{xii}$	180.0
O1–Rb1–$O1^{i}$	90.0	$O2^{xvi}$–Eu1–$O2^{xxii}$	80.05 (18)
$O1^{i}$–Rb1–$O1^{v}$	90.000 (2)	$O2^{xvi}$–Eu1–$O2^{xii}$	139.1 (5)
$O2^{xx}$–Eu1–$O2^{xxii}$	67.79 (17)	$O2^{xviii}$–Eu1–$O2^{xxii}$	112.21 (17)
$O2^{xxi}$–Eu1–$O2^{xxii}$	180.0	$O2^{xiv}$–Eu1–$O2^{xix}$	112.21 (17)
$O2^{xvii}$–Eu1–$O2^{xii}$	99.95 (18)	$O2^{xvi}$–Eu1–$O2^{xiii}$	112.21 (17)
$O2^{xiv}$–Eu1–$O2^{xiii}$	67.79 (17)	$O2^{xviii}$–Eu1–$O2^{xix}$	99.95 (18)
$O2^{xviii}$–Eu1–$O2^{xiii}$	40.9 (5)	$O2^{xxi}$–Eu1–$O2^{xix}$	139.1 (5)
$O2^{xx}$–Eu1–$O2^{xiii}$	139.1 (5)	$O2^{xii}$–Eu1–$O2^{xix}$	145.8 (3)
$O2^{xiii}$–Eu1–$O2^{xix}$	112.21 (17)	$O2^{xiv}$–Eu1–$O2^{xv}$	67.79 (17)

$O2^{xxi}$–Eu1–$O2^{xiii}$	34.2 (3)	$O2^{xxi}$–Eu1–$O2^{xv}$	40.9 (5)
O2–Eu1–$O2^{xvii}$	80.05 (18)	$O2^{xiii}$–Eu1–$O2^{xv}$	67.79 (17)
$O2^{xviii}$–Eu1–$O2^{xv}$	80.05 (18)	$O2^{xviii}$–Eu1–$O2^{xvii}$	139.1 (5)
$O2^{xiv}$–Eu1–$O2^{xvii}$	112.21 (17)	$O2^{xii}$–Eu1–$O2^{xv}$	34.2 (3)
O2–Eu1–$O2^{xiv}$	139.1 (5)	O2–Eu1–$O2^{xiii}$	99.95 (18)
$O2^{xix}$–Eu1–$O2^{xv}$	180.0	$O2^{xx}$–Eu1–$O2^{xix}$	80.05 (18)
$O2^{xx}$–Eu1–$O2^{xvii}$	40.9 (5)	O2–Eu1–$O2^{xix}$	34.2 (3)
$O2^{xxi}$–Eu1–$O2^{xvii}$	145.8 (3)	$O2^{xvi}$–Eu1–$O2^{xviii}$	145.8 (3)
O2–Eu1–$O2^{xvi}$	40.9 (5)	O2–Eu1–$O2^{xx}$	67.79 (17)
$O2^{xxi}$–Eu1–$O2^{xii}$	67.79 (17)	$O2^{xxii}$–Eu1–$O2^{xv}$	139.1 (5)
$O2^{xiv}$–Eu1–$O2^{xvi}$	180.0	$O2^{xviii}$–Eu1–$O2^{xx}$	180.0
$O2^{xvi}$–Eu1–$O2^{xv}$	112.21 (17)	$O2^{xiii}$–Eu1–$O2^{xii}$	80.05 (18)
O2–Eu1–$O2^{xviii}$	112.21 (17)	O2–Eu1–$O2^{xxi}$	112.21 (17)
$O2^{xiv}$–Eu1–$O2^{xii}$	40.9 (5)	$O2^{xviii}$–Eu1–$O2^{xii}$	67.79 (17)
$O2^{xiv}$–Eu1–$O2^{xx}$	145.8 (3)	$O2^{xvi}$–Eu1–$O2^{xx}$	34.2 (3)
$O2^{xiii}$–Eu1–$O2^{xvii}$	180.0		

Symmetry codes: (i) −*z*+1, −*x*+1, −*y*+1; (ii) *z*, *x*, *y*; (iii) −*y*+1, −*z*+1, −*x*+1; (iv) −*x*+1, −*y*+1, −*z*+1; (v) *y*, *z*, *x*; (vi) *y*+1/2, *z*, −*x*+3/2; (vii) −*x*+3/2, *y*+1/2, *z*; (viii) −*z*+1, *x*−1/2, −*y*+1/2; (ix) −*y*+1/2, −*z*+1, *x*−1/2; (x) *z*, −*x*+3/2, *y*+1/2; (xi) *x*−1/2, −*y*+1/2, −*z*+1; (xii) −*x*+1, −*y*+1, −*z*+2; (xiii) −*z*+3/2, −*y*+1, *x*+1/2; (xiv) *x*, −*z*+3/2, −*y*+3/2; (xv) −*y*+1, −*x*+1, −*z*+2; (xvi) −*x*+1, *z*−1/2, *y*+1/2; (xvii) *z*−1/2, *y*, −*x*+3/2; (xviii) −*y*+1, −*z*+3/2, −*x*+3/2; (xix) *y*, *x*, *z*; (xx) *y*, *z*−1/2, *x*+1/2; (xxi) −*z*+3/2, −*x*+1, −*y*+3/2; (xxii) *z*−1/2, *x*, *y*+1/2; (xxiii) *x*, −*y*+1/2, −*z*+3/2; (xxiv) −*x*+3/2, *y*, −*z*+3/2; (xxv) −*x*+3/2, −*y*+1/2, *z*; (xxvi) −*y*+1, −*x*+1, *z*; (xxvii) −*z*+3/2, −*x*+1, *y*+1/2; (xxviii) −*y*+1, *z*−1/2, −*x*+3/2; (xxix) −*x*+1, −*y*+1, *z*; (xxx) *x*+1/2, *y*−1/2, *z*.

2–293 K

Eu1–O2	2.556 (10)	Rb1–O1	2.824 (16)
$O2^{i}$–Eu1–$O2^{iv}$	180.0	$O2^{i}$–Eu1–$O2^{viii}$	34.3 (4)
$O2^{ix}$–Eu1–$O2^{v}$	90.000 (2)	$O2^{i}$–Eu1–$O2^{ii}$	40.8 (6)
$O2^{viii}$–Eu1–$O2^{ix}$	112.2 (2)	$O2^{iv}$–Eu1–$O2^{viii}$	145.7 (4)

$O2^{i}$–Eu1–$O2^{vi}$	67.8 (2)	$O2^{xii}$–Eu1–$O2^{ii}$	34.3 (4)
$O2^{x}$–Eu1–$O2^{ii}$	100.0 (2)	$O2^{vi}$–Eu1–$O2^{viii}$	40.8 (6)
$O2^{iv}$–Eu1–$O2^{vi}$	112.2 (2)	$O2^{vii}$–Eu1–$O2^{ix}$	112.2 (2)
$O2^{iv}$–Eu1–$O2^{v}$	49.2 (6)	$O2^{i}$–Eu1–$O2^{x}$	112.2 (2)
$O2^{iii}$–Eu1–$O2^{v}$	100.0 (2)	$O2^{i}$–Eu1–$O2^{xi}$	112.2 (2)
$O2^{iv}$–Eu1–$O2^{x}$	67.8 (2)	$O2^{iv}$–Eu1–$O2^{ix}$	40.8 (6)
$O2^{iii}$–Eu1–$O2^{xii}$	139.2 (6)	$O2^{iv}$–Eu1–$O2^{xi}$	67.8 (2)
$O2^{vi}$–Eu1–$O2^{x}$	180.0	$O2^{xi}$–Eu1–$O2^{ix}$	34.3 (4)
$O2^{vi}$–Eu1–$O2^{ii}$	80.0 (2)	$O2^{vi}$–Eu1–$O2^{xi}$	112.2 (2)
$O2^{viii}$–Eu1–$O2^{x}$	139.2 (6)	$O2^{ii}$–Eu1–$O2^{ix}$	180.0
$O2^{iii}$–Eu1–$O2^{ii}$	112.2 (2)	$O2^{viii}$–Eu1–$O2^{xi}$	100.0 (2)
$O2^{x}$–Eu1–$O2^{v}$	67.8 (2)	$O2^{iv}$–Eu1–$O2^{ii}$	139.2 (6)
$O2^{x}$–Eu1–$O2^{xi}$	67.8 (2)	$O2^{viii}$–Eu1–$O2^{iii}$	112.2 (2)
$O2^{xii}$–Eu1–$O2^{v}$	67.8 (2)	$O2^{viii}$–Eu1–$O2^{ii}$	67.8 (2)
$O2^{i}$–Eu1–$O2^{iii}$	100.0 (2)	$O2^{x}$–Eu1–$O2^{iii}$	34.3 (4)
$O2^{xi}$–Eu1–$O2^{xii}$	180.0	$O2^{xi}$–Eu1–$O2^{ii}$	145.7 (4)
$O2^{iv}$–Eu1–$O2^{iii}$	80.0 (2)	$O2^{xi}$–Eu1–$O2^{iii}$	40.8 (6)
$O2^{vii}$–Eu1–$O2^{xii}$	40.8 (6)	$O2^{vii}$–Eu1–$O2^{ii}$	67.8 (2)
$O2^{vi}$–Eu1–$O2^{iii}$	145.7 (4)	$O2^{i}$–Eu1–$O2^{vii}$	80.0 (2)
$O2^{i}$–Eu1–$O2^{ix}$	139.2 (6)	$O2^{xii}$–Eu1–$O2^{ix}$	145.7 (4)
$O2^{iv}$–Eu1–$O2^{vii}$	100.0 (2)	$O2^{xi}$–Eu1–$O2^{vii}$	139.2 (6)
$O2^{vi}$–Eu1–$O2^{ix}$	100.0 (2)	$O2^{i}$–Eu1–$O2^{v}$	130.8 (6)
$O2^{vi}$–Eu1–$O2^{vii}$	34.3 (4)	$O2^{iii}$–Eu1–$O2^{vii}$	180.0
$O2^{x}$–Eu1–$O2^{ix}$	80.0 (2)	$O2^{viii}$–Eu1–$O2^{v}$	145.7 (4)
$O2^{viii}$–Eu1–$O2^{vii}$	67.8 (2)	$O2^{i}$–Eu1–$O2^{xii}$	67.8 (2)
$O2^{iii}$–Eu1–$O2^{ix}$	67.8 (2)	$O2^{xi}$–Eu1–$O2^{v}$	112.2 (2)
$O2^{x}$–Eu1–$O2^{vii}$	145.7 (4)	$O2^{iv}$–Eu1–$O2^{xii}$	112.2 (2)
$O2^{vii}$–Eu1–$O2^{v}$	80.0 (2)	O1–Rb1–$O1^{xv}$	90.000 (1)

$O2^{vi}$–Eu1–$O2^{xii}$	67.8 (2)	$O1^{xvi}$–Rb1–$O1^{xvii}$	90.000 (1)
$O2^{ii}$–Eu1–$O2^{v}$	90.000 (2)	$O1^{xvi}$–Rb1–$O1^{xiii}$	90.000 (1)
$O2^{viii}$–Eu1–$O2^{xii}$	80.0 (2)	O1–Rb1–$O1^{xvi}$	90.000 (3)
$O2^{x}$–Eu1–$O2^{xii}$	112.2 (2)	O1–Rb1–$O1^{xiii}$	90.000 (1)
$O2^{vi}$–Eu1–$O2^{v}$	112.2 (2)	$O1^{xv}$–Rb1–$O1^{xvi}$	180.0
$O1^{xv}$–Rb1–$O1^{xvii}$	90.000 (1)	$O1^{xiv}$–Rb1–$O1^{xiii}$	90.000 (1)
O1–Rb1–$O1^{xiv}$	180.0	O1–Rb1–$O1^{xvii}$	90.0
$O1^{xiv}$–Rb1–$O1^{xvii}$	90.000 (1)	$O1^{xvii}$–Rb1–$O1^{xiii}$	180.0
$O1^{xv}$–Rb1–$O1^{xiv}$	90.000 (2)	$O1^{xvi}$–Rb1–$O1^{xiv}$	90.000 (1)
$O1^{xv}$–Rb1–$O1^{xiii}$	90.000 (1)		

Symmetry codes: (i) −*z*+1, −*y*+2, *x*; (ii) −*y*+3/2, −*z*+3/2, −*x*+1; (iii) *z*, *x*+1/2, *y*−1/2; (iv) *z*, *y*, −*x*+1; (v) −*z*+1, *y*, −*x*+1; (vi) *x*, −*z*+3/2, −*y*+3/2; (vii) −*z*+1, −*x*+3/2, −*y*+3/2; (viii) −*x*+1, −*y*+2, −*z*+1; (ix) *y*−1/2, *z*+1/2, *x*; (x) −*x*+1, *z*+1/2, *y*−1/2; (xi) *y*−1/2, *x*+1/2, *z*; (xii) −*y*+3/2, −*x*+3/2, −*z*+1; (xiii) −*z*+1, −*x*+1, −*y*+1; (xiv) −*x*+1, −*y*+1, −*z*+1; (xv) −*y*+1, −*z*+1, −*x*+1; (xvi) *y*, *z*, *x*; (xvii) *z*, *x*, *y*; (xviii) *x*, −*y*+1, *z*; (xix) −*x*+1, −*y*+1, *z*; (xx) −*x*+1, *y*, −*z*+1; (xxi) −*x*+1, *y*, *z*; (xxii) *x*, *y*, −*z*+1; (xxiii) −*x*+1/2, −*y*+3/2, *z*; (xxiv) −*x*+1/2, *y*, −*z*+1/2; (xxv) *x*, −*y*+3/2, −*z*+1/2.

3–311 K

Eu1–O2	2.580 (7)	Eu2–O20	2.561 (6)
Eu1–O3	2.568 (7)	Eu2–O21	2.598 (7)
Eu1–O5	2.601 (7)	Eu2–O23	2.585 (6)
Eu1–O6	2.581 (6)	Eu2–O24	2.603 (7)
Eu1–O7	2.608 (7)	Eu2–O26	2.576 (6)
Eu1–O8	2.565 (6)	Eu2–O27	2.575 (6)
Rb1–O1	2.894 (7)	Rb2–O13	2.855 (7)
Rb2–O19	2.906 (7)	$O25^{ix}$–Rb2–$O16^{viii}$	80.9 (3)
O2–Eu1–O5	67.6 (2)	$O25^{ix}$–Rb2–O19	83.9 (3)
O3–Eu1–O2	49.4 (2)	O19–Rb2–$O4^{vi}$	113.0 (2)
O5–Eu1–O7	66.9 (2)	O19–Rb2–$O9^{vii}$	108.6 (2)
O6–Eu1–O5	48.7 (2)	$O25^{ix}$–Rb2–$O4^{vi}$	154.2 (2)

O8–Eu1–O5	68.3 (2)	$O25^{ix}$–Rb2–$O9^{vii}$	115.8 (3)
O11–Eu1–O3	67.6 (2)	$O1^{ii}$–Rb1–O1	180.0
O12–Eu1–O2	111.5 (2)	O1–Rb1–$O22^{v}$	68.1 (2)
O14–Eu1–O5	110.8 (2)	O1–Rb1–$O22^{i}$	111.9 (2)
O15–Eu1–O2	112.6 (2)	$O1^{ii}$–Rb1–$O22^{v}$	111.9 (2)
O15–Eu1–O6	68.2 (2)	$O1^{ii}$–Rb1–$O22^{i}$	68.1 (2)
O15–Eu1–O7	178.9 (2)	$O10^{iii}$–Rb1–O1	84.9 (3)
O17–Eu1–O5	67.4 (2)	$O10^{iv}$–Rb1–O1	95.1 (3)
O17–Eu1–O7	110.5 (2)	$O10^{iv}$–Rb1–$O1^{ii}$	84.9 (3)
O18–Eu1–O2	179.5 (2)	$O10^{iii}$–Rb1–$O1^{ii}$	95.1 (3)
O18–Eu1–O3	130.8 (2)	$O10^{iv}$–Rb1–$O10^{iii}$	180.0 (5)
O18–Eu1–O5	112.4 (2)	$O10^{iii}$–Rb1–$O22^{v}$	76.5 (3)
O18–Eu1–O6	111.6 (2)	$O10^{iii}$–Rb1–$O22^{i}$	103.5 (3)
$O20^{i}$–Eu2–O20	180.0	$O10^{iv}$–Rb1–$O22^{v}$	103.5 (3)
O20–Eu2–O21	49.2 (2)	$O10^{iv}$–Rb1–$O22^{i}$	76.5 (3)
O21–Eu2–$O21^{i}$	180.0	$O22^{i}$–Rb1–$O22^{v}$	180.0 (3)
O21–Eu2–O24	68.0 (2)	$O4^{vi}$–Rb2–$O9^{vii}$	78.5 (2)
O23–Eu2–O21	113.6 (2)	O13–Rb2–$O4^{vi}$	89.7 (3)
$O23^{i}$–Eu2–O21	66.4 (2)	O13–Rb2–$O9^{vii}$	167.7 (2)
O24–Eu2–$O24^{i}$	180.00 (17)	O13–Rb2–$O16^{viii}$	86.8 (3)
O26–Eu2–$O21^{i}$	112.4 (2)	O13–Rb2–O19	79.2 (3)
O26–Eu2–O23	70.8 (2)	O13–Rb2–$O25^{ix}$	73.8 (3)
O26–Eu2–O21	67.6 (2)	$O16^{viii}$–Rb2–$O4^{vi}$	78.4 (3)
O26–Eu2–O24	67.2 (2)	O27–Eu2–O23	113.9 (2)
O26–Eu2–$O26^{i}$	180.0 (4)	O27–Eu2–O24	113.2 (2)
O27–Eu2–O21	70.4 (2)	O27–Eu2–O26	49.4 (2)
O27–Eu2–$O27^{i}$	180.0		

Symmetry codes: (i) −*x*, −*y*+1, −*z*; (ii) −*x*, −*y*, −*z*; (iii) *x*−1, *y*, *z*; (iv) −*x*+1, −*y*, −*z*; (v) *x*, *y*−1, *z*; (vi) −*x*+1, −*y*+1, −*z*+1; (vii) *x*, *y*+1, *z*; (viii) −*x*+2, −*y*+1, −*z*+1; (ix) −*x*+1, −*y*+1, −*z*; (x) *x*+1, *y*, *z*.

Table S5. Anisotropic displacement parameters ($Å^2 \times 10^3$) for **1** ,**2** and **3**.

	U_{11}	U_{22}	U_{33}	U_{12}	U_{13}	U_{23}
1–193 K						
N1	0.151 (6)	0.151 (6)	0.151 (6)	–0.0001 (7)	0.0154 (9)	0.0000 (7)
O3	0.151 (6)	0.151 (6)	0.151 (6)	–0.0001 (8)	0.0153 (10)	0.0000 (8)
N3	0.131 (7)	0.131 (7)	0.131 (7)	0.0000 (8)	0.0134 (11)	0.0000 (8)
N2	0.065 (5)	0.065 (5)	0.065 (5)	0.000	0.0067 (9)	0.000
O5	0.065 (5)	0.065 (5)	0.065 (5)	0.0000 (7)	0.0067 (10)	0.0000 (7)
O4	0.066 (5)	0.066 (5)	0.065 (5)	0.000	0.0067 (10)	0.000
O6	0.065 (5)	0.065 (5)	0.065 (5)	0.0000 (7)	0.0067 (10)	0.0000 (7)
O1	0.151 (6)	0.151 (6)	0.151 (6)	–0.0001 (7)	0.0154 (10)	0.0000 (7)
O2	0.151 (6)	0.151 (6)	0.151 (6)	–0.0001 (7)	0.0154 (10)	0.0000 (7)
1–293 K						
O1	0.104 (6)	0.083 (5)	0.048 (3)	0.000	0.000	–0.020 (3)
O2	0.177 (8)	0.177 (8)	0.073 (6)	0.000	0.000	0.000
N1	0.088 (4)	0.088 (4)	0.056 (5)	0.000	0.000	0.000
2–293 K						
O1	0.31 (2)	0.033 (7)	0.31 (2)	0.000	0.000	0.000
O2	0.130 (9)	0.062 (6)	0.095 (8)	0.000	0.000	–0.027 (5)
N1	0.128 (9)	0.038 (7)	0.128 (9)	0.000	0.000	0.000
3-311 K						
O1	0.044 (4)	0.064 (5)	0.061 (5)	−0.003 (4)	−0.017 (4)	0.013 (4)
O2	0.042 (4)	0.052 (4)	0.049 (4)	0.006 (3)	0.011 (3)	0.016 (3)
O3	0.045 (4)	0.056 (4)	0.043 (4)	0.005 (3)	0.009 (3)	0.019 (3)
O4	0.066 (5)	0.070 (5)	0.054 (4)	0.029 (4)	0.042 (4)	0.022 (4)
O5	0.049 (4)	0.049 (4)	0.042 (4)	0.015 (3)	0.018 (3)	0.020 (3)
O6	0.049 (4)	0.045 (4)	0.048 (4)	0.011 (3)	0.021 (3)	0.018 (3)
O7	0.042 (4)	0.041 (4)	0.054 (4)	0.006 (3)	0.011 (3)	0.022 (3)
O8	0.046 (4)	0.040 (4)	0.047 (4)	0.006 (3)	0.007 (3)	0.021 (3)
O9	0.084 (6)	0.039 (4)	0.075 (5)	0.006 (4)	0.014 (4)	0.037 (4)
O10	0.107 (7)	0.082 (6)	0.087 (6)	0.039 (6)	0.079 (6)	0.038 (5)
O11	0.054 (4)	0.044 (4)	0.050 (4)	0.012 (3)	0.023 (3)	0.021 (3)
O12	0.058 (4)	0.046 (4)	0.055 (4)	0.018 (3)	0.029 (3)	0.022 (3)
O13	0.097 (7)	0.041 (4)	0.110 (7)	0.018 (4)	0.026 (6)	0.053 (5)

O14	0.050 (4)	0.058 (4)	0.056 (4)	0.013 (4)	0.010 (3)	0.034 (4)
O15	0.050 (4)	0.045 (4)	0.056 (4)	0.007 (3)	0.010 (3)	0.025 (3)
O16	0.041 (4)	0.097 (7)	0.058 (5)	−0.004 (4)	−0.013 (4)	0.028 (5)
O17	0.040 (4)	0.060 (4)	0.039 (4)	0.002 (3)	0.010 (3)	0.015 (3)
O18	0.042 (4)	0.048 (4)	0.047 (4)	0.011 (3)	0.013 (3)	0.022 (3)
O19	0.038 (4)	0.073 (5)	0.063 (5)	0.012 (4)	−0.015 (4)	0.006 (4)
O20	0.044 (4)	0.040 (4)	0.034 (3)	0.012 (3)	0.010 (3)	0.007 (3)
O22	0.114 (7)	0.028 (4)	0.058 (5)	0.002 (4)	0.022 (5)	0.016 (3)
O23	0.051 (4)	0.037 (3)	0.033 (3)	0.009 (3)	0.010 (3)	0.012 (3)
O24	0.054 (4)	0.040 (4)	0.048 (4)	0.002 (3)	0.007 (3)	0.017 (3)
O25	0.093 (7)	0.120 (8)	0.064 (5)	0.059 (6)	0.057 (5)	0.056 (5)
O26	0.056 (4)	0.050 (4)	0.054 (4)	0.018 (3)	0.030 (3)	0.028 (3)
O27	0.042 (4)	0.049 (4)	0.047 (4)	0.020 (3)	0.018 (3)	0.022 (3)
N1	0.056 (4)	0.048 (4)	0.045 (4)	0.013 (4)	0.015 (3)	0.022 (3)
N2	0.058 (5)	0.073 (5)	0.050 (4)	0.022 (4)	0.015 (4)	0.040 (4)
N3	0.042 (4)	0.043 (4)	0.044 (4)	0.016 (3)	0.017 (3)	0.019 (3)
N4	0.033 (4)	0.031 (4)	0.034 (4)	−0.001 (3)	−0.003 (3)	0.009 (3)
N5	0.036 (4)	0.043 (4)	0.028 (4)	0.010 (3)	0.010 (3)	0.012 (3)
N6	0.040 (4)	0.033 (4)	0.046 (4)	0.008 (3)	0.020 (4)	0.022 (3)
N7	0.043 (4)	0.047 (5)	0.042 (4)	0.007 (4)	0.024 (4)	0.018 (4)
N8	0.047 (5)	0.031 (4)	0.052 (5)	0.005 (4)	0.019 (4)	0.019 (4)
N9	0.031 (4)	0.037 (4)	0.033 (4)	0.001 (3)	−0.001 (3)	0.016 (3)
N10	0.040 (5)	0.029 (4)	0.039 (4)	0.004 (3)	−0.003 (4)	0.002 (3)
N11	0.058 (5)	0.028 (4)	0.038 (4)	0.008 (4)	0.020 (4)	0.013 (3)
N12	0.034 (4)	0.071 (6)	0.035 (4)	0.021 (4)	0.015 (3)	0.028 (4)

$$\Delta S = \int_{T_1}^{T_2} \frac{Q}{T} dT \approx \frac{\Delta H}{T} = \frac{10.6437\ J \cdot g^{-1} \times 826.68\ g \cdot mol^{-1}}{252.5\ K} = \frac{8798.93\ J \cdot mol^{-1}}{252.5\ K} \approx \cdot K^{-1}$$

$$\Delta S = R \ln N$$

$$N = \exp\left(\frac{\Delta S}{R}\right) = \exp\left(\frac{34.8472\ J \cdot mol^{-1} \cdot K^{-1}}{8.314\ J \cdot mol^{-1} \cdot K^{-1}}\right) = 66.1145$$

$$\Delta S = \int_{T_1}^{T_2} \frac{Q}{T} dT \approx \frac{\Delta H}{T} = \frac{13.4963\, J \cdot g^{-1} \times 893.41\, g \cdot mol^{-1}}{276.5\, K} = \frac{12057.73\, J \cdot mol^{-1}}{276.5\, K} \cdot K^{-1}$$

$$\Delta S = R \ln N$$

$$N = \exp\left(\frac{\Delta S}{R}\right) = \exp\left(\frac{43.6084\, J \cdot mol^{-1} \cdot K^{-1}}{8.314\, J \cdot mol^{-1} \cdot K^{-1}}\right) = 189.6493$$

$$\Delta S = \int_{T_1}^{T_2} \frac{Q}{T} dT \approx \frac{\Delta H}{T} = \frac{9.0515\, J \cdot g^{-1} \times 1009.56\, g \cdot mol^{-1}}{324.6\, K} = \frac{9138.03\, J \cdot mol^{-1}}{324.6\, K} \approx \cdot K^{-1}$$

$$\Delta S = R \ln N$$

$$N = \exp\left(\frac{\Delta S}{R}\right) = \exp\left(\frac{28.1517\, J \cdot mol^{-1} \cdot K^{-1}}{8.314\, J \cdot mol^{-1} \cdot K^{-1}}\right) = 29.5493$$

References

1. J. J. Ma, Q. Xu, L. Ye, Q. W. Wang, Z. X. Gong, C. Shi, H. Y. Zhang and Y. Zhang, Structural phase transition and dielectric switching in an organic-inorganic hybrid rare-earth double perovskite-type compound: $(DMP)_2LaRb(NO_3)_6$ (DMP = N,N-dimethylpyrrolidinium cation), *J. Rare Earths*., 2022, **40**, 937−941.
2. Q. Xu, L. Ye, R. M. Liao, Z. An, C. F. Wang, L. P. Miao and Y. Zhang, H/F Substitution induced large increase of T_c in a 3D hybrid rare-earth double perovskite multifunctional compound, *Chem. Eur. J*., 2022, **28**, e202103913.
3. D. F. Li, F. Guo, X. L. He, Y. Z. Wu, X. H. Deng, K. P. Yang, and Y. X. Li, A layered hybrid rare-earth double perovskite with two continuous reversible phase transitions induced by unusual two driving gears of fan-like rotation movements, *CrystEngComm*, 2022, **24**, 8496−8502.
4. Q. Q. Jia, H. F. Lu, J. Q. Luo, Y. Y. Zhang, H. F. Ni, F. W. Zhang and Y. Zhang, Organic-inorganic rare-rarth double perovskite ferroelectric with large piezoelectric response and ferroelasticity for flexible composite energy harvesters, *Small*., 2024, **20**, 2306989.
5. C. Shi, J. J. Ma, J. Y. Jiang, M. M. Hua, Q. Xu, H. Yu, Y. Zhang and H. Y. Ye, Large piezoelectric response in hybrid rare-earth double perovskite relaxor ferroelectrics, *J. Am. Chem. Soc*., 2020, **142**, 9634−9641.
6. Z. B. Hu, C. F. Wang, T. T. Sha, C. Shi, L. Ye, H. Y. Ye, Y. Song, Y. M. You and Y.

Zhang, An effective strategy of introducing chirality to achieve multifunctionality in rare-earth double perovskite ferroelectrics, *Small Methods*, 2022, **6**, 2200421.

7. C. F. Wang, C. Shi, A. Y. Zheng, Y. L. Wu, L. Ye, N. Wang, H. Y. Ye, M. J. Ju, P. F. Duan, J. L. Wang and Y. Zhang, Achieving circularly polarized luminescence and large piezoelectric response in hybrid rare-earth double perovskite by a chirality induction strategy, *Mater. Horiz*., 2022, **9**, 2450−2459.
8. C. Shi, L. Ye, Z. X. Gong, J. J. Ma, Q. W. Wang, J. Y. Jiang, M. M. Hua, C. F. Wang, H. Yu, Y. Zhang and H. Y. Ye, Two-dimensional organic-inorganic hybrid rare-earth double perovskite ferroelectrics, *J. Am. Chem. Soc*., 2020, **142**, 545−551.
9. Q. H. Zou, Z. J. Wang, L. K. Wu, Y. Feng, L. L. Jiang, J. R. Li and C. Shi, Three-Dimensional bimetallic ammonium K-Eu nitrate with a rare (6,6)-connected ion topology exhibiting structural phase transition and photoluminescence properties. *Inorg. Chem*., 2024, doi: 10.1021/acs.inorgchem.4c01520.
10. Z. J. Wang, L. H. Li, Y. Feng, Q. W. Wang, L. K. Wu, J. R. Li and H. Y. Ye, Synthesis, dielectric, magnetic, and photoluminescence properties of two new hybrid rare-earth double perovskites, *Front. Chem*., 2022, **10**, 969156.
11. M. M. Hua, L. Ye, Q. W. Wang, J. J. Ma, Z. X. Gong, Q. Xu, C. Shi and Y. Zhang, A layered hybrid rare-earth double-perovskite-type molecule-based compound with electrical and optical response properties, *J. Mater. Chem. C*., 2020, **8**, 16349−16353.